

Exploring Spatial Segregation Induced by Competition Avoidance as Driving Mechanism for Emergent Coexistence in Microbial Communities

Mattia Mattei¹ and Alex Arenas^{1,2}

¹*Departament d'Enginyeria Informàtica i Matemàtiques,
Universitat Rovira i Virgili, 43007 Tarragona, Spain*

²*Pacific Northwest National Laboratory, 902 Battelle Blvd, Richland, WA, 99354, USA*

This study investigates the role of spatial segregation, prompted by competition avoidance, as a key mechanism for emergent coexistence within microbial communities. Recognizing these communities as complex adaptive systems, we challenge the sufficiency of pairwise interaction models and consider the impact of spatial dynamics. We developed an individual-based spatial simulation depicting bacterial movement through a pattern of random walks influenced by competition avoidance, leading to the formation of spatially segregated clusters. This model was integrated with a Lotka-Volterra metapopulation framework focused on competitive interactions. Our findings reveal that spatial segregation alone can lead to emergent coexistence in microbial communities, offering a new perspective on the formation of stable, coexisting microbe clusters that differ significantly from their behavior in isolated pairwise interactions. This study underscores the importance of considering spatial factors in understanding the dynamics of microbial ecosystems.

I. INTRODUCTION

Microorganisms do not function in isolation; rather, they exist within multi-species communities, cohabiting the same environment and engaging in a spectrum of complex interactions. This complexity poses a substantial challenge in understanding how the physiological behaviors of individual species contribute to emergent properties such as stability, productivity, and resilience. From this perspective, microbial communities can be regarded as ‘*complex adaptive systems*’ [1], making them well-suited for rigorous quantitative theoretical analysis. Indeed, a plethora of mathematical models have been applied to describe the microbiome. These range from variations of the Lotka-Volterra equations [2] and MacArthur’s consumer-resource model [3, 4] to frameworks based on evolutionary game theory [5], among others.

Recently, Chang et al. [6] presented solid experimental proofs that multispecies coexistence is an *emergent phenomenon*: they isolated organisms from stable synthetic bacterial communities consisting of various species and competed all possible combination of pairs of organisms to test their ability to live together; in most cases, one species outcompeted the other, leading to exclusion. From this, they concluded that coexistence in communities cannot be reduced to pairwise coexistence rules and they left open the question about the fundamental mechanisms behind it. In particular, they wonder whether the complex nature of multispecies coexistence derives from higher-order interactions (HOIs), or whether it can be explained by a complex network of pairwise relations.

Providing a precise definition of HOIs, particularly in the field of ecology, is challenging [7]. One possible simplified conceptualization is to view HOIs as a modifications of pairwise interactions in the presence of a third or more species. The research by Mickalide and Kuehn [8] reveals a HOI aligning with this definition. An ‘in-

teraction modification’ unfolds, wherein a single-celled algae (*Chlamydomonas reinhardtii*) alters the dynamics between a predatory ciliate (*Tetrahymena thermophila*) and the bacterium *E. coli*. This modification stems from a phenotypic change in *E. coli* triggered by the presence of *C. reinhardtii*; the algae inhibits the aggregation of *E. coli* cells, rendering them more susceptible to predation by the ciliate.

In general, it is always possible to generalize mathematical models to incorporate groups interactions [9], but identifying the various and often intricate driving physical mechanisms behind them can be demanding. Before employing such sophisticated tools and concepts, we wonder whether the simpler framework of complex networks of pairwise interactions is sufficient to explain the emergent phenomena.

Studies such as those conducted by Thebault and Fontaine [10] or Rohr et al. [11] have illustrated how the architecture of the network of pairwise interactions among species significantly influences the stability and overall macroscopic characteristics of an ecosystem. In this context, a pertinent question emerges: why, within the same ecosystem, do certain species interact among them while others do not? Perhaps the most straightforward explanation lies in how species are *spatially distributed*.

There is abundant evidence indicating the significance of spatial constraints in the formation of microbial communities and the emergence of spatially segregated clusters of bacteria. For instance, Welch et al. [12] discovered highly organized spatial structure in the oral microbiome and a surprising correlation between position in space of taxa and their function. Conwill et al. [13] showed how lineages with in vitro fitness differences coexist within centimeter-scale regions on human skin, but each skin pore being dominated by a single lineage. Shi et al. [14] developed a new technology for mapping the microbiome and they discovered that microbial communities in oral biofilms are spatially structured as stable mi-

croarchitectures over time. Cho et al. [15], through the utilization of an innovative microfluidic device, showed that bacterial colonies of *E. Coli* have the capability to autonomously self-organize within chambers of varying shapes and sizes that permit continuous cell escape. In general, colonies of bacteria exhibit a fascinating propensity to form tight structures in various settings in response to unfavorable environmental conditions including various types of chemical stress [16].

The core concept of this study is to explore the potential of spatial self-organization among microbes as the underlying factor contributing to the observed emergent coexistence identified by Chang et al. To achieve this objective, it is necessary to develop a model that simulates bacterial movement. Bacteria in a liquid medium exhibit a movement pattern characterized by alternating between tumble and swim phases [17]. In a uniform environment, the movement of a bacterium resembles a random walk, with relatively straight swimming segments occasionally interrupted by random tumbles that reorient the bacterium. Notably, bacteria such as *E. coli* lack the ability to deliberately choose their swimming direction and cannot maintain a straight path for an extended period due to rotational diffusion, essentially “forgetting” their trajectory. To compensate for this, they continuously assess their course and make adjustments when necessary, allowing them to steer their random walk towards favorable locations. This movement of bacteria in response to chemical gradient is called *chemotaxis*.

While it may be reasonable to attribute bacterial movements primarily to nutrient-driven research, it is essential to acknowledge that chemotaxis is both imprecise and energetically costly for bacteria, especially in densely populated environments (Brumley [18]). Additionally, when considering bacterial communities in batch cultures in vitro, such as those studied by Chang et al., there is no clear reason to assume uneven nutrient distribution or strong nutrient gradients influencing bacterial motion. A more plausible proposition would be that the predominant driving force behind bacterial movement is an unoriented escape response from highly competitive environments to less competitive ones, facilitated by a uniform distribution of nutrients.

Following this direction, we developed an individual-based spatial simulation to depict the individual movement of bacteria, leading to the formation of spatially segregated clusters resulting from the *escape* from regions with high competition. This simulation was then utilized to calculate the initial conditions for a metapopulations Lotka-Volterra model with only competitive interactions, capturing the growth dynamics of such patches of bacteria. This study shows that: i) segregation of clusters of bacteria can be obtained as a result of competition avoidance only and, therefore, it can potentially occur in any conditions regardless of the environmental setup; ii) considering a metapopulation structure in a Lotka-Volterra formalism alters considerably the pattern of coexistence for the species and iii) spatial segregation and bacterial

self-organization can be seen as the driving mechanisms behind the emergence observed by Chang et al., i.e. the formation of stable coexisting small microbial communities, the majority of which do not coexist when isolated in pairwise combinations. As a benchmark to validate our model, we also confirmed its ability to replicate the three macroecological laws governing microbial communities, as discovered by J. Grilli[19].

II. INDIVIDUAL-BASED SPATIAL SIMULATION FOR BACTERIAL MOTION

The simulation starts by uniformly distributing n bacteria within a two-dimensional square and subsequently randomly assigning each of them to one of $N < n$ different species. While other initial spatial distributions are conceivable—such as placing bacteria of the same species in closer proximity—these variations do not appear to influence the final results. Hence, we opted to proceed with the initially uniform distribution for its generality. We can then assume that each cell interacts only with the cells in its proximity. If we think about bacteria as nodes in a network, the simple formalism of Random Geometric Graph (RGG) [20] can be employed to rapidly evaluate the number of bacteria in the neighborhood of each node. In a RGG two nodes are connected when their distance is within a certain neighborhood radius R . Here, the euclidean distance is considered, i.e. two nodes i and j are connected when $d_{ij} = \sqrt{(x_i - x_j)^2 + (y_i - y_j)^2} < R$. The idea is that the higher the density of competitors in the vicinity of node i the more it is inclined to escape from that region. Therefore, we update nodes positions according to:

$$\begin{cases} x_i(t+1) = x_i(t) + I_i(t) \cos \theta_i(t), \\ y_i(t+1) = y_i(t) + I_i(t) \sin \theta_i(t), \end{cases} \quad (1)$$

with θ_i uniformly distributed between $[0, 2\pi]$ at each time-step and

$$I_i(t) = \frac{R}{1 + e^{-\alpha \left(\frac{N_c^i(t)}{N_{th}} - 1 \right)}}. \quad (2)$$

In other words we model bacterial movement selecting a random direction and an intensity proportional to the level of competitiveness, i.e. the number of competitors N_c^i in the neighborhood of the node i . Taking inspiration from neural networks, the intensity of motion is modelled as a sigmoid function (figure 1). The parameter α controls the the shape of the curve; if $\alpha \rightarrow \infty$ the function tends to the Heaviside step-function. The threshold parameter N_{th} controls the position of the inflection point $N_c^i = N_{th}$. This function cannot be equal to zero, disallowing bacteria to be completely still, and its maximum value is equal to R , i.e. the radius of the neighborhood area.

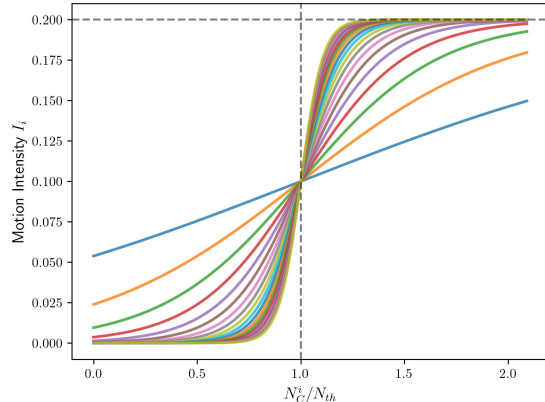


FIG. 1. **The function for the bacterial intensity of motion.**

Each curve is described by equation 2 with different α between 1 and 20. The greater α , the more the function tends to a step function. Here, R is chosen equal to 0.2.

The simulation stops when all the bacteria minimize their intensity motion, i.e. when their activity results in a random walk confined in a small portion of space. As we will see later, it is always possible to choose the parameters (α, N_{th}) to ensure that this formalism naturally generates spatially segregated clusters of bacteria, whose dimensions depends on the radius of interactions R .

In order to quantitatively compute the different clusters of bacteria in the final network we employed the classical Louvain Algorithm for communities detection [21]. It optimizes a quality function known as modularity, which quantifies the strength of the community structure in a network. The algorithm optimizes modularity by iteratively moving nodes between communities, enhancing the overall cohesion within communities while reducing connectivity between them. The Louvain algorithm is a popular choice in the field of network science, despite the numerous limitations associated with modularity optimization algorithms [22]. In our context, the selection of a particular algorithm has negligible effects.

III. A DIFFUSIVE LOTKA-VOLTERRA METAPOPULATION MODEL

The Lotka-Volterra equations are the gold standard to model the dynamics of interacting populations in ecology [23]. In the generalized version for N species, they can reproduce each possible type of relations according to the sign of the interactions matrix entries, from competition to cooperation. A growing debate surrounds the significance of positive interactions among bacterial species. Numerous studies, as the one by Palmer and Foster [24], showed that negative interactions tend to predominate, and instances of cooperation, where two species mutually benefit, are generally infrequent. Contrary findings are

presented in studies such as that of Kehe et al. [25], wherein positive interactions, particularly parasitisms, are identified as common occurrences, especially among strains exhibiting distinct carbon consumption profiles. In this work, we have opted for the exclusive incorporation of negative interactions in Lotka-Volterra equations. We posit that the simpler and more justified assumption lies in considering competition for nutrients as the primary environmental-mediated interactions shaping bacterial populations.

Given the initial setup involves spatially separated bacterial clusters, adopting a metapopulation model proves advantageous. Metapopulation models are frameworks in ecology that conceptualize the dynamics of interconnected populations within a fragmented landscape. Coined by Richard Levins [26], the metapopulation concept views a population as a set of subpopulations occupying discrete patches of habitat, with occasional migration or dispersal occurring between these patches. The dynamics of each subpopulation are influenced by local factors like birth, death, and interactions, as well as the exchange of individuals among patches. Ngoc et al. offer an illustration of Lotka-Volterra formalism tailored for metapopulation in their work [27]. Their model explores the dynamics of two species in competition for an implicit resource within a habitat divided into two patches.

In this work we have adapted the Lotka-Volterra formalism as follows:

$$\begin{aligned} \frac{dX_{i\alpha}(t)}{dt} = & r_i X_{i\alpha}(t) \left(1 - \frac{1}{K_i} \sum_{j \in \alpha} A_{ij} X_{j\alpha}(t) \right) \\ & + \mu_d \sum_{\beta} M_{\alpha\beta} (X_{i\beta}(t) - X_{i\alpha}(t)) \end{aligned} \quad (3)$$

where the Latin indices refer to species while the Greek ones to the different N_p patches; thus, $X_{i\alpha}$ represents the population of species i in patch α . The intrinsic growth rate and the carrying capacity of species i are indicated as r_i and K_i respectively. The interaction coefficient A_{ij} depends only on the species types i and j and the sum in the first term runs over all the species j placed in patch α , i.e. species interact only if in the same patch. Moreover, in this formulation the entries of \mathbf{A} are all positive in order to reproduce only competitive interactions. The coefficient μ_d modulates the diffusion term. The matrix \mathbf{M} represents the network connecting the patches, obtained from the last random geometric graph provided by the simulation. In particular, $M_{\alpha\beta} = m_{\alpha\beta}/n_{\alpha}n_{\beta}$ with $m_{\alpha\beta}$ number of links between the communities and n_{α} , n_{β} number of nodes in α and β respectively. In summary, the weights $M_{\alpha\beta}$ quantify the proximity between different patches.

A. On the stability of Lotka-Volterra equations

As μ_d approaches 0, the equilibrium solutions within each patch become well-established and are solely de-

pendent on the interaction pattern and carrying capacities, given by $X_{i\alpha}^* = \sum_{j \in \alpha} (\mathbf{A}^{-1})_{ij} K_j$. It is recognized that for global stability of the feasible fixed point ($X_{i\alpha}^* > 0 \ \forall i, \alpha$), the matrix \mathbf{A} must be negative definite. In other words, $\mathbf{A} + \mathbf{A}^T$ should possess exclusively negative eigenvalues, as thoroughly explained by Grilli et al. in their study [28]. In his groundbreaking research [29], Robert May demonstrated that large ecological networks exhibit a notably low probability of stability. Specifically, when matrix entries are sampled from a random distribution with a mean of zero and a mean square value of α , the system is almost certain to be unstable if $\alpha > 1/\sqrt{N}$. Building upon May's findings, Allesina and Tang [30] extended the results differentiating between the various types of relationships, including predator-prey, competition, or mutualism. They provided analytical stability criteria for each scenario. The key takeaway from these insights is that in the case of competition, system stability is only assured when there is a predominant presence of very weak interactions.

Mathematical analyses of stability typically focus on conditions near equilibrium points due to analytical challenges in dealing with nonlinear systems at a distance from equilibrium. For this reason, Holling [31] suggested defining the behavior of ecological systems with two distinct properties: resilience and stability. Resilience pertains to the persistence of relationships within a system and measures its ability to absorb changes in state variables, driving variables, and parameters while still persisting. Stability, on the other hand, refers to a system's capacity to return to equilibrium after a temporary disturbance, with a more rapid and less fluctuating return indicating greater stability. The well-known *mutual invasion criterion*, often associated with the concept of resilience, serves as a notable benchmark. For stable coexistence, it demands that each species within a community demonstrates positive population growth rates when invading a pre-existing community of competitors from low density [32]. This is exactly the indicator used by Chang et al. to assess stable coexistence in their experimental communities of microbial species. Take a moment to focus on a scenario involving only two species within the system. In the context of competitive Lotka-Volterra equations, it is established that the invasion criterion holds true when $A_{12} < K_1/K_2$ and $A_{21} < K_2/K_1$ [33]. Consequently, note that weak interactions with zero mean would almost always satisfy the invasion criterion and, consequently, lead to stable coexistence. However, Chang et al. [6] observed in their experiments that only a relatively small fraction (about 30%) of possible pairs of species complies with the invasion criterion. When contemplating the parameters A_{ij} as 'universal' coefficients for pairwise interactions, it appears that these experimental results are scarcely consistent with the conditions necessary for mathematical asymptotic stability. The work by Abramson and Zanette [34], provides us a workaround. They randomly selected interaction coefficients for a system comprising N Lotka-Volterra species

from a uniform distribution centered around one. Remarkably, the resulting phase space exhibited a multitude of fixed points, with a majority featuring both positive and negative eigenvalues—indicating instability. Consequently, the system traverses various unstable equilibria, leading to instances where the population of certain species undergoes pseudo-extinctions, reaching very low concentrations before rebounding. The noteworthy finding in their study is the demonstration that introducing a lower bound, X_0 , to the populations induces a shift in the stability of nearly all equilibria, transforming them into stable states. It is important to note that the imposition of a lower threshold on populations is entirely justified. Indeed, the population density of a species or genotype confined to a specific spatial volume V cannot fall below V^{-1} unless it disappears entirely. When describing densities, it becomes essential to establish a threshold below which the density effectively approaches zero. They additionally demonstrated that enlarging the domain from which interaction coefficients are sampled results in a reduction in the number of species surviving at equilibrium. All of these heuristic discussions provide compelling justifications for our parameter choices in the model, which will be detailed in the results section. Moreover, we recall that our theoretical setup incorporates the structural aspect of patches, a factor that significantly influences coexistence and stability requirements. The next section will provide further clarification on this point.

B. Mesoscopic Interpretation of the Interactions Parameters

Let's consider the dynamics for the entire population $X_i = \sum_{\alpha} X_{i\alpha}$ of the species rather than focusing on the subpopulations in individual patches. If we express the population of species i in terms of fractions ϕ ranging from 0 to 1 (i.e., $X_i(t) = \phi_{i\alpha}(t)X_{i\alpha}(t)$), we obtain the following equation:

$$\frac{dX_i(t)}{dt} = r_i X_i(t) \left(1 - \frac{1}{K_i} \sum_{\alpha, j} \phi_{i\alpha}(t) A_{ij} \phi_{j\alpha}(t) X_j(t) + \frac{\mu_d}{r_i} \sum_{\alpha, \beta} M_{\alpha\beta} (\phi_{i\beta}(t) - \phi_{i\alpha}(t)) \right). \quad (4)$$

Being the metapopulation network undirected, i.e. $M_{\alpha\beta} = M_{\beta\alpha}$, the last term of equation above is zero. Indeed, the migration between patches does not affect the global population. To recover the standard Lotka-Volterra equations for entire populations, we define

$$A_{ij}^G(t) \equiv A_{ij} S_{ij}(t) = A_{ij} \sum_{\alpha}^{N_p} \phi_{i\alpha}(t) \phi_{j\alpha}(t).$$

Here, S_{ij} , ranging between 0 and 1, measures the *proximity* between species i and j , i.e. the extent of segre-

gation between them, indicating how much they occupy the same patches. When they don't share any patches, S_{ij} is zero; when their entire populations are in the same patch, $S_{ij} = 1$. This interpretation of the global interaction parameters A_{ij}^G combines the 'true' strength of interaction A_{ij} between two species with the mesoscale spatial distribution across patches. It's noteworthy that even two strongly interacting species with a high A_{ij} can have a limited global impact on each other if they are adequately segregated in space. Indeed, the proximity measure changes the solutions at equilibrium which now have to satisfy

$$\sum_j (\mathbf{S}^* \odot \mathbf{A})_{ij} X_j^* = K_i. \quad (5)$$

Let's see how the invasion criterion in the case of two species changes in this new fashion. Suppose that species 1 is rare, $X_1 \sim 0$, while species 2 is at equilibrium X_2^* :

$$\begin{aligned} \frac{dX_2^*}{dt} &= r_2 X_2^* \left(1 - \frac{1}{K_2} \sum_{\alpha} (\phi_{2\alpha}^*)^2 A_{22} X_2^* \right) \\ &= 0 \Leftrightarrow X_2^* = \frac{K_2}{A_{22} \sum_{\alpha} (\phi_{2\alpha}^*)^2}. \end{aligned} \quad (6)$$

The species 1 will be able to invade the system if $dX_1(t)/dt > 0$, i.e. if

$$A_{12} < \frac{K_1}{K_2} \frac{\sum_{\alpha} (\phi_{2\alpha}^*)^2}{\sum_{\alpha} \phi_{1\alpha} \phi_{2\alpha}^*} \equiv \frac{K_1}{K_2} \Omega_{21}, \quad (7)$$

where we have considered $A_{ii} = 1$. To comply with the mutual invasion criterion the same must hold also for A_{21} , inverting the indices. However species 2, in absence of species 1, has grown equally in all the patches until equilibrium; this means that $\phi_{2\alpha}^* = 1/N_p$, $\forall \alpha$. Considering also that $\sum_{\alpha} \phi_{1\alpha} = 1$, we obtain that the factor Ω is equal to one and we revert to the classical invasion criterion conditions. Therefore, this elucidates how the mesoscale structure can at the same time relevantly affect the global interactions A_{ij}^G , and so the steady state, for species in communities while maintaining the same conditions for pairwise stable coexistence in the sense of the invasion criterion.

C. Grilli's Macroecological Laws

A recent contribution by J. Grilli [9] represents a significant stride in the macroecological exploration of microbial communities. Through the analysis of data from different biomes, the study delineates patterns of abundance variation, encapsulating three macroecological laws: i) the abundance fluctuations of any given species across samples adhere to a gamma distribution; ii) the variances of these distributions for distinct species are proportional to the square of their means, known as Taylor's law [35]; and iii) the mean abundances across species conform to a

lognormal distribution. He also showed how a Stochastic Logistic Model (SLM), which enhances a logistic growth with a multiplicative stochastic term reproducing environmental effects, can perfectly reproduce the phenomenology. In an even more recent work by Camacho-Mateu et al. [36] a generalized stochastic Lotka-Volterra model (SLVM) was introduced, incorporating pairwise interactions. This model was also able to uphold Grilli's three empirical laws. They considered only weak interactions in order to comply with the global stability of the feasible fixed point requirements. We will demonstrate that our framework can replicate Grilli's laws, even when accounting for stronger interactions and incorporating information about environmental stochasticity within our spatial simulation.

IV. RESULTS

We conducted multiple runs of our spatial simulation, considering $n = 2000$ bacteria, i.e. nodes in the RGG, assigned to $N = 100$ different species and exploring various values of the radius R and threshold N_{th} . Remarkably, for each radius value, it is always possible to find a corresponding N_{th} such that the simulation reaches a form of equilibrium relatively quickly. This equilibrium comprises different spatially segregated clusters of bacteria, where each bacterium attains a very low velocity of motion and predominantly occupies a single patch. Figure 2 presents two simulation runs with $R = 0.2, 0.3$ and $N_{th} = 60, 160$, respectively in panel a) and b). In the former, snapshots of the system at different time steps are displayed alongside the associated intensity motion distribution. As the nodes cluster, the distribution shifts towards very low values. In panel b), we illustrate how increasing R leads to the formation of larger clusters. In the last two snapshots of b) and in panel c), we illustrate how the modularity optimization Louvain algorithm successfully identifies distinct communities, clearly revealing the different patches. All the simulations are performed in 2×2 bidimensional square. It's important to note that the range of velocities considered is biologically plausible: bacteria can move at a wide range of speeds ranging from $1 \mu\text{m/s}$ to $1000 \mu\text{m/s}$ [37]; considering the square as $2 \times 2 \text{ mm}^2$, this implies that bacteria at the beginning of our simulation travel on average $141 \mu\text{m}$ in a few seconds of straight-line motion, with a maximum possible value of about $280 \mu\text{m}$; then, at the end of simulation, they all reach velocities of very few μm per second.

Upon reaching equilibrium, each simulation yields the initial distribution of various species across patches, representing the initial conditions in our metapopulation model for species growth. We numerically solved the system of differential equations using an explicit Runge-Kutta method of order 5. For simplicity, we opted for identical and unitary intrinsic growth rates and carrying capacities for all species ($K_i = 1$, $r_i = 1$, $\forall i$). In light of section 3.1, we chose not to require asymptotic stability

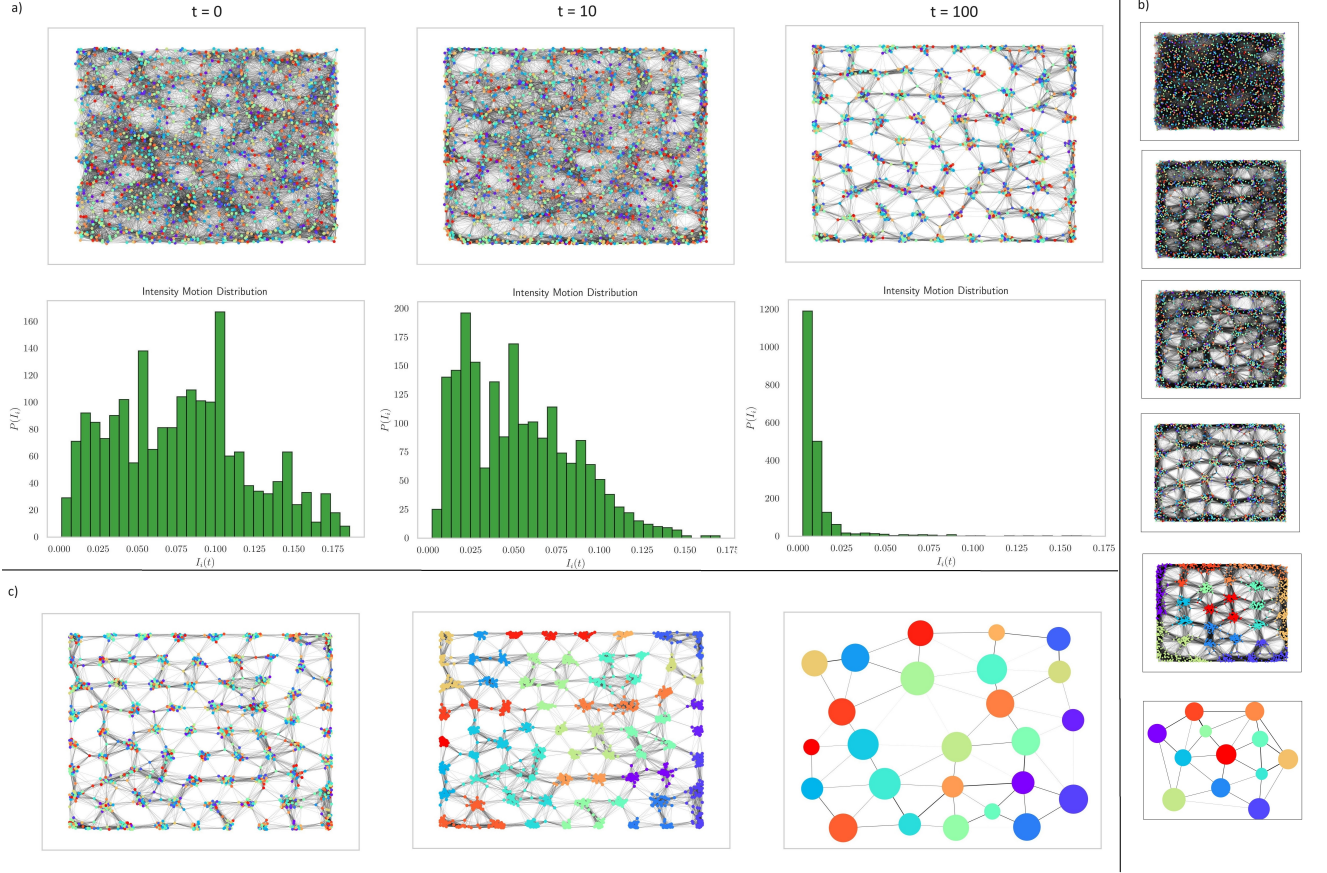


FIG. 2. **Emergence of Spatially Segregated Bacterial Clusters Resulting from Competition Avoidance.**

The simulation in panel a) was conducted with $R = 0.2$ and $N_{th} = 60$. We considered $n = 2000$ nodes randomly assigned to $N = 100$ different species, each one distinguished by a different color. The top row presents the random geometric network representation of the system, while the bottom row illustrates the intensity motion distribution. In the smaller panel b), the graph at different time steps is shown for $R = 0.3$ and $N_{th} = 160$. The last two snapshots in b) and panel c) show the application of the Louvain algorithm to the RGG at the equilibrium, identifying the different patches. The dimension of the patches is proportional to the number of nodes within them and the widths of the edges are chosen accordingly to the number of links between the respective communities. All simulations are performed in a two-dimensional square of dimensions 2×2 .

but to follow a direction similar to Abramson et al. [34], therefore we randomly sampled the off-diagonal entries of the interaction matrix from a lognormal distribution with a mean (μ) set to one, varying its variance (σ^2) from 0.1 to 0.5 ($A_{ij} \sim \text{Lognormal}(\mu, \sigma)$). The lognormal distribution was chosen in order to sample only positive A_{ij} . The diagonal elements were uniformly set to one ($A_{ii} = 1$). Additionally, we incorporated a lower limit for the population, denoted as $X_{i\alpha}^0$, set at 10^{-6} . Furthermore, we explored various values for the diffusion parameter (μ_d), spanning from zero to approximately 10^2 .

In Figure 3, we present an illustrative instance of species dynamics from a single model run. Specifically, the main plot exhibits the dynamics and attainment of equilibrium (we considered the system exhibits equilibrium dynamics if the coefficient of variation for the entire population of species was below 1% in the last 500 time-steps) for the total populations of the species, while the top inset illustrates the dynamics for the individual

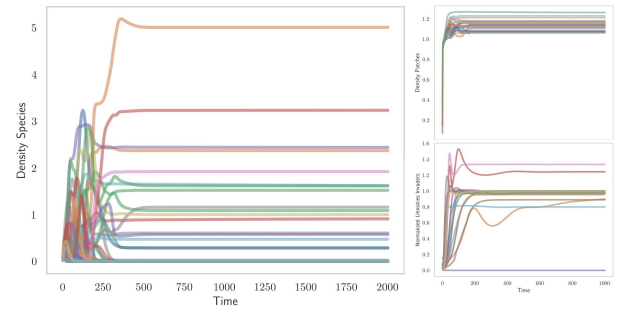


FIG. 3. **Species' dynamics**

The primary plot illustrates the temporal dynamics of the overall population of the species, while the top inset depicts the dynamics at the level of individual patches. The bottom inset displays the dynamics of the 'invaders' when assessing the invasion criterion; the abundances are normalized by their previous levels at equilibrium.

patches. In each model run, we assessed whether the resulting equilibrium could be deemed ‘stable’ according to the invasion criterion, i.e., we significantly reduced the population of each surviving species and observed whether they returned to similar levels as before. In every simulation, we consistently found that over 90% of the species were capable of successfully re-invading the system. An illustration is presented in the bottom inset, depicting the populations of the invaders normalized by their previous concentrations. They all rebound to a value close to one, except for a solitary species that dies due to its initially very low concentration.

The first set of simulations consisted in 100 runs for three different values of σ (0.1, 0.3 and 0.5) and with μ_d fixed to 10. Once the system exhibits equilibrium, we checked the number of survived species. Subsequently, we examined all possible pairs of survivors and re-executed the simulation with only these two species in the system, using the same interaction parameters as before. Following the approach in Chang et al., we investigated whether the two species coexisted at equilibrium, considering three different initial distribution percentages: 50%-50%, 95%-5%, and 5%-95%. In picture 4 we show the results for the number of survivors (top row) and for the percentage of pairs of survivors that coexist in isolation (bottom row). The number of survivors is always much higher than that expected in the case of classical Lotka-Volterra model with the same parameters but without patches structure, which, therefore, facilitates coexistence among species. This can be explained looking to the fractions ϕ_i before and after executing the model. Specifically, refer to figure 5 to observe the ‘proximity measure’ S_{ij} for each pair of species both before and after allowing them to grow and migrate. In the initial state, S_{ij} exhibits a bell-shaped distribution, indicating that the spatial simulation results in species that are, on average, evenly segregated among the patches. Following the model execution, the surviving species demonstrate a distribution more concentrated around zero and with a long tail, suggesting that survivors are more likely to be highly segregated with a small minority of them being able to coexist in the same patches. This phenomenon facilitates the coexistence of species, even when their net interaction A_{ij} is high.

Conversely, we found that only a minority of couples of species (about 32%) coexist when isolated, resembling the experimental results and reproducing the emergent behaviour (figure 4, bottom row). In fact, in the absence of multiple species, spatial self-organization in this scenario leads to a random process distributing both species equally across all patches with high probability, as depicted in figure 6. This implies an unaffected interaction pattern, rendering the spatial distribution incapable of promoting coexistence. When there is a significant disparity in the initial concentration of the two species, as previously mentioned, the patch structure does not impact the invasion criterion when one species invades the other. Consequently, the mesoscale structure, while

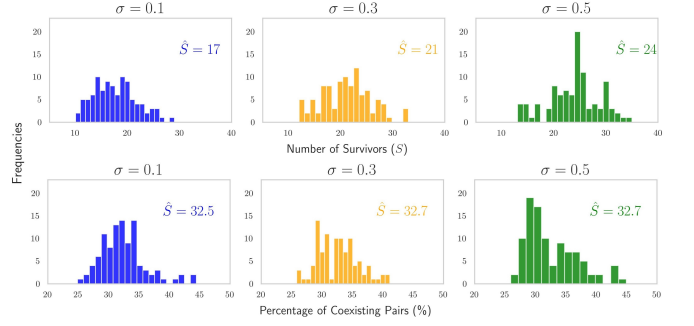


FIG. 4. **Distributions for the number of survivors and the percentage of those capable of coexisting when isolated.**

The distributions were obtained after 100 runs of the spatial simulation and the metapopulation model for three different values of the interactions standard deviation $\sigma = 0.1, 0.3, 0.5$. In each simulation, we verified the count of surviving species (top row) and subsequently isolated every potential pair to assess their coexistence in the pairwise configuration. The bottom row displays the distribution of the corresponding percentages. For all the simulations $n = 2000$, $N = 100$, $R = 0.2$, $N_{th} = 60$, $K_i = 1$ and $r_i = 1 \forall i$, $\mu_d = 10$, $X_{i\alpha}^0 = 10^{-6} \forall (i, \alpha)$.

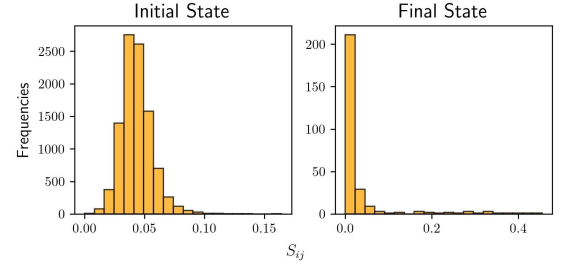


FIG. 5. **Proximity Measures**

Distribution of the proximity measure S_{ij} for each pair of species, before and after species’ growth and over 100 runs of the complete model. In the final state we considered all possible couples of only survived species.

potentially influencing coexistence in multi-species configurations, does not change the criteria for coexistence in the case of two species. This elucidates the findings illustrated in Figure 4.

It can be argued that the value of the diffusion parameter μ_d , representing the extent to which species migrate across patches, can exert a significant influence on the ultimate number of surviving species by potentially reducing segregation among species. To investigate this, we conducted multiple model runs while keeping the parameters constant, except for μ_d . As depicted in Figure 7, an increase in μ_d corresponds to a lower number of survivors, as expected. However, beyond a certain value of μ_d , the number of survivors reaches a plateau and no longer decreases. Hence, the metapopulation structure continues to enhance coexistence compared to the classical global Lotka-Volterra model, irrespective of the diffusion factor.

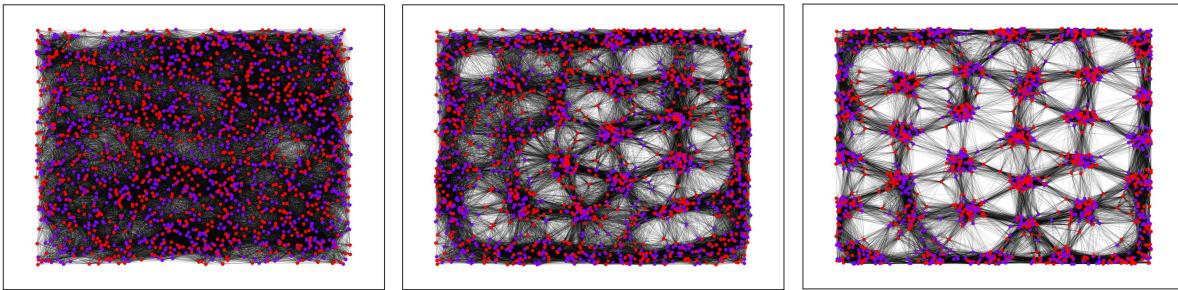


FIG. 6. **Individual Spatial Simulation of Two Species at Various Stages.**

The spatial simulation displays two distinct species at the initial, intermediate, and final stages, progressing from left to right. The latter presents the two species uniformly mixed in each patch. In this instance, parameters were set as follows: $R = 0.3$, $\alpha = 7$, and $N_{th} = 160$.

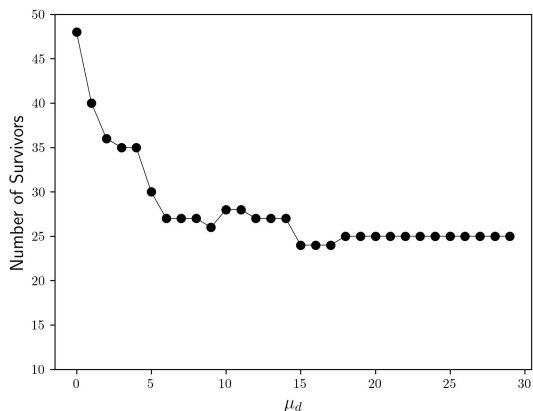


FIG. 7. **Number of survived species varying the diffusion factor.**

We checked the number of survivors for multiple runs of the model maintaining the same parameters except for μ_d which varies from 0 to 10^2 . The other parameters were chosen as described in the caption of figure 4.

As mentioned earlier, a robust testing ground for a model aspiring to describe the microbiome involves verifying its ability to replicate the three macroecological laws outlined in section 3.3. To achieve this, we conducted multiple model runs each time changing the interactions, simulating various samples of the same system. Subsequently, we examined the abundance distribution of species across samples (Abundance Fluctuation Distribution, AFD), the relationship between the variance and mean of species abundances, and the distribution of mean abundances across species (Mean Abundance Distribution, MAD). All these analyses demonstrated good agreement with the patterns identified by Grilli (see Figure 8), resulting in R^2 values of 0.98, 0.47, and 0.88, respectively, for the three laws. The second law exhibits less alignment with theoretical expectations. Nevertheless, recent findings [38] strongly indicate that the second

law cannot be regarded as a precise relationship between mean and variance. Instead, the exponent appears to be sampled from a distribution rather than remaining a constant, leading to increased dispersion in data points, as observed in our case. This hypothesis finds support in both empirical observations and the predictions of an approximate theory.

V. DISCUSSION

In this study, we have developed a theoretical framework that combines an individual-based spatial simulation of bacterial motion with a metapopulation Lotka-Volterra model to describe abundance dynamics. The current model has demonstrated its capability to replicate certain experimental phenomena, such as the intriguing emergence of coexistence observed by Chang et al. Specifically, the model facilitates coexistence in multi-species systems by fostering the spatial rearrangement of bacteria into distinct clusters. This spatial segregation is a consequence of a high escape response triggered when the local environment becomes densely populated and competitive. The self-organization into different patches consistently leads to a greater number of bacteria surviving, as spatial separation limits interactions among them. However, this process proves to be less efficient in the case of a two-species system. When two species have a strong interaction, the only viable way to coexist is complete segregation within the system. If bacteria are uniformly distributed, there is a high probability that both species will end up in each patch, therefore not changing the pattern of competition.

One could posit that the described phenomenon occurs because bacteria, when assessing the density of surrounding competitors, are unable to discriminate between different species. This leads to the inclusion of cells from the same species as perceived competitors. However, there is no inherent reason to assume any form of cooperation between bacteria of the same species. As mentioned earlier, cooperation, although possible, tends to be infrequent

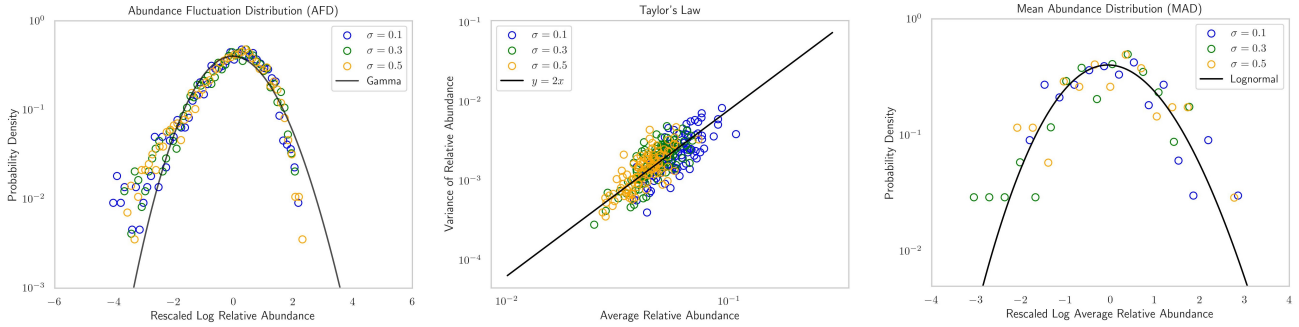


FIG. 8. **Grilli's macroecological laws.**

We conducted multiple model runs, sampling different interactions A_{ij} in each simulation. A total of 100 runs were performed for three distinct values of σ (0.1, 0.3, and 0.5). Subsequent to all the simulations, we assessed whether the species' abundances across runs followed a gamma distribution (left figure), if the mean and variance of the abundances were related through Taylor's law with an exponent of two (central figure), and finally, if the mean abundance was distributed according to a lognormal distribution (right figure). The analysis resulted in R^2 values of 0.98, 0.47, and 0.88, respectively, for the three laws. The various colors of the circles represent the three values of σ . The remaining parameters in the model were selected as in Figure 4.

both among bacteria of the same species and across different species [24, 39, 40]. This rationale underlies our decision to exclusively consider negative interactions in the formulation of the growth model.

Similarly, it can be argued that the absence of uneven nutrient distribution in our model may impose limitations on its applicability. Nevertheless, when considering experimental communities, they are typically cultured in agar plates or batch cultures where nutrients are generally thoroughly mixed, resulting in a uniform distribution throughout the medium. Given this context, we assume that there is no substantial nutrient concentration gradient influencing bacterial motion. Thus, we posit that the predominant driving force for movement is the avoidance of competition and we showed how even in isotropic environments with no particular nutrients distribution, is still possible to have a spatial structure with meta-communities, affecting the coexistence among species. A consumer-resource model would necessitate making various assumptions about nutrient abundances, types, temporal dynamics, spatial distribution, and more. The Lotka-Volterra formalism allows the modeling of resource competition without delving into specific resource details. In Chang et al.'s experiments, nutrients start off limited, leading to bacterial competition. However, the nutrients undergo repeated replenishment throughout multiple cycles. If we consider the experiment duration significantly exceeds the duration of a single cycle, it is akin to assuming an overall stable nutrient concentration. Consequently, even if a different model, like MacArthur's Consumer-Resource model incorporating nutrient dynamics, were employed, assuming globally constant nutrient concentrations over time would essentially reduce it to a formalism equivalent to Lotka-Volterra dynamics.

Bacteria rank among the fastest reproducers globally, doubling at the scale of minutes [41]. However, their

motion is also remarkably rapid, with swimming speeds exceeding 100 body lengths per second [42, 43]. This substantiates our assumption of effectively separating the temporal scales between self-organization in space and growth.

While numerous instances of empirical evidence support bacterial self-organization in space, our model currently lacks experimental validation. Nevertheless, we have shown that our theoretical framework aligns with the three macroecological laws identified by J. Grilli, providing a form of empirical confirmation. Efforts are underway to experimentally validate our assumptions and to scale the model for increased biological plausibility. Future endeavors will involve a significantly higher number of bacteria situated in a three-dimensional space with varied geometry, a task currently beyond reach due to the computational power at our disposal.

In summary, our objective with this work is to convey a fundamental message — that space distribution is a crucial factor. Particularly in ecological theoretical models, the common approach involves a mean-field approximation, assuming that each species interacts with all others in the system. While a completely microscopic approach may pose challenges, our study demonstrates that incorporating a mesoscale structure, such as distinct communities or patches in space, can profoundly influence the dynamics and coexistence patterns. Simultaneously, we illustrated how minimal adaptability levels can lead to the formation of isolated bacterial clusters, maintaining a high degree of randomness that mirrors the intricate stimuli influencing bacterial motion. We believe that this work has the potential to pave the way for a new research direction, emphasizing the importance of considering the delicate spatial equilibrium between species within a microbial community as a pivotal element to be incorporated into theoretical models and investigations.

AUTHOR CONTRIBUTIONS STATEMENT

A.A. and M.M. designed the study; M.M. performed simulations, mathematical calculations and data analysis; A.A. supervised the results; A.A. and M.M. wrote and approved the manuscript.

ACKNOWLEDGEMENTS

This project has received funding from the European Union’s Horizon 2020 research and innovation pro-

gramme under the Marie Skłodowska-Curie grant agreement No. 945413 and from the Universitat Rovira i Virgili (URV).

COMPETING INTERESTS

The authors declare no conflict of interest.

-
- [1] Hyun-Seob Song, William R. Cannon, Alexander S. Beliaev, and Allan Konopka. Mathematical modeling of microbial community dynamics: A methodological review. *Processes*, 2(4):711–752, 2014.
 - [2] Katharine Z. Coyte, Jonas Schluter, and Kevin R. Foster. The ecology of the microbiome: Networks, competition, and stability. *Science*, 350(6261):663–666, 2015.
 - [3] Joshua E. Goldford, Nanxi Lu, Djordje Bajić, Sylvie Estrela, Mikhail Tikhonov, Alicia Sanchez-Gorostiaga, Daniel Segrè, Pankaj Mehta, and Alvaro Sanchez. Emergent simplicity in microbial community assembly. *Science*, 361(6401):469–474, 2018.
 - [4] Anna Posfai, Thibaud Taillefumier, and Ned S. Wingreen. Metabolic trade-offs promote diversity in a model ecosystem. *Phys. Rev. Lett.*, 118:028103, Jan 2017.
 - [5] Erwin Frey. Evolutionary game theory: Theoretical concepts and applications to microbial communities. *Physica A: Statistical Mechanics and its Applications*, 389(20):4265–4298, 2010. Proceedings of the 12th International Summer School on Fundamental Problems in Statistical Physics.
 - [6] Chang-Yu Chang, Djordje Bajić, Jean C. C. Vila, Sylvie Estrela, and Alvaro Sanchez. Emergent coexistence in multispecies microbial communities. *Science*, 381(6655):343–348, 2023.
 - [7] Alvaro Sanchez. Defining higher-order interactions in synthetic ecology: Lessons from physics and quantitative genetics. *Cell Systems*, 9(6):519–520, 2019.
 - [8] Harry Mickalide and Seppe Kuehn. Higher-order interaction between species inhibits bacterial invasion of a phototroph-predator microbial community. *Cell Systems*, 9(6):521–533.e10, 2019.
 - [9] J. Grilli, G. Barabás, and M. Michalska-Smith et al. Higher-order interactions stabilize dynamics in competitive network models. *Nature*, 548:210–213, 2017.
 - [10] Elisa Thébault and Colin Fontaine. Stability of ecological communities and the architecture of mutualistic and trophic networks. *Science*, 329(5993):853–856, 2010.
 - [11] Rudolf P. Rohr, Serguei Saavedra, and Jordi Bascompte. On the structural stability of mutualistic systems. *Science*, 345(6195):1253497, 2014.
 - [12] Jessica L. Mark Welch, Blair J. Rossetti, Christopher W. Rieken, Floyd E. Dewhirst, and Gary G. Borisy. Biogeography of a human oral microbiome at the micron scale. *Proceedings of the National Academy of Sciences*, 113(6):E791–E800, 2016.
 - [13] Conwill A., Kuan AC, and Damerla R. et al. Anatomy promotes neutral coexistence of strains in the human skin microbiome. *Cell Host Microbe*, 30:171–182, 2022.
 - [14] H. Shi, Q. Shi, and B. Grodner et al. Highly multiplexed spatial mapping of microbial communities. *Nature*, 588:676–681, 2020.
 - [15] HoJung Cho, Henrik Jönsson, Kyle Campbell, Pontus Melke, Joshua W Williams, Bruno Jedynak, Ann M Stevens, Alex Groisman, and Andre Levchenko. Self-organization in high-density bacterial colonies: Efficient crowd control. *PLOS Biology*, 5(11):1–10, 10 2007.
 - [16] L. Hall-Stoodley, J. Costerton, and P. Stoodley. Bacterial biofilms: from the natural environment to infectious diseases. *Nat Rev Microbiol*, 2:95–108, 2004.
 - [17] H. Berg and D. Brown. Chemotaxis in escherichia coli analysed by three-dimensional tracking. *Nature*, 239:500–504, 1972.
 - [18] DR. Brumley, F. Carrara, AM. Hein, Y. Yawata, SA. Levin, and R. Stocker. Bacteria push the limits of chemotactic precision to navigate dynamic chemical gradients. *Proc Natl Acad Sci U S A.*, 116(22):410792–10797, 2019.
 - [19] Grilli J. Macroecological laws describe variation and diversity in microbial communities. *Nat Commun*, 11:4743, 2020.
 - [20] Mathew Penrose. *Random Geometric Graphs*. Oxford University Press, 05 2003.
 - [21] Vincent D Blondel, Jean-Loup Guillaume, Renaud Lambiotte, and Etienne Lefebvre. Fast unfolding of communities in large networks. *Journal of Statistical Mechanics: Theory and Experiment*, 2008(10):P10008, oct 2008.
 - [22] Tiago P. Peixoto. Hierarchical block structures and high-resolution model selection in large networks. *Phys. Rev. X*, 4:011047, Mar 2014.
 - [23] Vito Volterra. Variations and Fluctuations of the Number of Individuals in Animal Species living together. *ICES Journal of Marine Science*, 3(1):3–51, 04 1928.
 - [24] Jacob D. Palmer and Kevin R. Foster. Bacterial species rarely work together. *Science*, 376(6593):581–582, 2022.
 - [25] Jared Kehe, Anthony Ortiz, Anthony Kulesa, Jeff Gore, Paul C. Blainey, and Jonathan Friedman. Positive interactions are common among culturable bacteria. *Science Advances*, 7(45):eabi7159, 2021.
 - [26] Richard Levins. Some Demographic and Genetic Consequences of Environmental Heterogeneity for Biological Control. *Bulletin of the Entomological Society of America*, 15(3):237–240, 09 1969.

- [27] Doanh Nguyen Ngoc, Rafael Bravo de la Parra, Miguel A. Zavala, and Pierre Auger. Competition and species coexistence in a metapopulation model: Can fast asymmetric migration reverse the outcome of competition in a homogeneous environment? *Journal of Theoretical Biology*, 266(2):256–263, 2010.
- [28] J. Grilli, M. Adorisio, and S. Suweis et al. Feasibility and coexistence of large ecological communities. *Nat Commun*, 8:14389, 2017.
- [29] R. May. Will a large complex system be stable? *Nature*, 238:413–414, 1972.
- [30] S. Allesina and S. Tang. Stability criteria for complex ecosystems. *Nature*, 483:205–208, 2012.
- [31] C. S. Holling. Resilience and stability of ecological systems. *Annual Review of Ecology and Systematics*, 4:1–23, 1973.
- [32] Tess Nahanni Grainger, Jonathan M. Levine, and Benjamin Gilbert. The invasion criterion: A common currency for ecological research. *Trends in Ecology & Evolution*, 34(10):925–935, 2019.
- [33] Robert Macarthur and Richard Levins. The limiting similarity, convergence, and divergence of coexisting species. *The American Naturalist*, 101(921):377–385, 1967.
- [34] Guillermo Abramson and Damián H. Zanette. Statistics of extinction and survival in lotka-volterra systems. *Phys. Rev. E*, 57:4572–4577, Apr 1998.
- [35] L. Taylor. Aggregation, variance and the mean. *Nature*, 189:732–735, 1961.
- [36] José Camacho-Mateu, Aniello Lampo, Matteo Sireci, Miguel Ángel Muñoz, and José A. Cuesta. Sparse species interactions reproduce abundance correlation patterns in microbial communities, 2023.
- [37] HC. Berg. The rotary motor of bacterial flagella. *Annu Rev Biochem*, 72:19–54, 2003.
- [38] Jose Cuesta. Private communication with the author, pending proper referencing upon publication. 2024.
- [39] ME. Hibbing, C. Fuqua, MR. Parsek, and SB. Peterson. Tbacterial competition: surviving and thriving in the microbial jungle. *Nat Rev Microbiol*, 8(1):15–25, 2010.
- [40] KR. Foster and T. Bell. Competition, not cooperation, dominates interactions among culturable microbial species. *Curr Biol*, 22(19):1845–1850, 2012.
- [41] RJ. Allen and B. Waclaw. Bacterial growth: a statistical physicist’s guide. *Rep Prog Phys*, 82(1), 2019.
- [42] J G Mitchell, L Pearson, and S Dillon. Clustering of marine bacteria in seawater enrichments. *Applied and Environmental Microbiology*, 62(10):3716–3721, 1996.
- [43] Rolf H. Luchsinger, Birger Bergersen, and James G. Mitchell. Bacterial swimming strategies and turbulence. *Biophysical Journal*, 77(5):2377–2386, 1999.